Accepted manuscript in the *Journal of Sound and Vibration*

Ultrasonic interference and critical attenuation in metal-plastic bilayer laminates

Naoki Mori*, Takahiro Hayashi

Department of Mechanical Engineering, Graduate School of Engineering, Osaka University

2-1 Yamadaoka, Suita, Osaka 565-0871, Japan.

* Corresponding author.

E-mail address: n.mori@mech.eng.osaka-u.ac.jp (N. Mori)

ABSTRACT

The resonance of ultrasonic waves in a metal-plastic bilayer laminate placed in an infinite medium is theoretically investigated, and critical attenuation is shown to occur under specific conditions. The bilayer laminate is subjected to normal wave incidence from the side of the plastic layer. Based on a linear viscoelastic model, the amplitude of the reflection spectrum for the laminate is formulated to obtain the exact results for wave resonance and critical attenuation by numerical calculations. Furthermore, the approximate formulae for the conditions of the resonance and critical attenuation are derived explicitly by Taylor expansions with respect to the loss factor of the plastic. As a result, the exact solution shows that the resonance frequencies of the plastic layer slightly increase with increasing loss factor. Their variation with the loss factor agrees well with the second-order approximation result but is insignificant in the cases of common plastics with relatively low loss factors. The exact results also show that the amplitude at each order resonance depends on the loss factor and has a minimum at a critical loss factor. The obtained critical loss factor decreases with increasing resonance order and is well reproduced by the zeroth-order approximation. Experiments are performed on two types of metal-plastic bonded laminates, demonstrating that the measured reflection spectra are in good agreement with the theoretical predictions. In particular, the amplitude of the measured reflection spectrum decreases significantly at a resonance frequency, which is theoretically predicted to satisfy the critical attenuation condition.

Keywords: Layered structure; Interference; Critical attenuation; Reflection; Viscoelasticity

1. Introduction

Elastic wave propagation in layered structures is one of the classical issues in acoustics [1, 2], yielding fundamental knowledge for various applications, e.g., the design of acoustic devices and the ultrasonic spectroscopy of laminates. A basic case is that an elastic wave impinges on a single planar layer placed in an infinite medium. For the normal incidence of a plane wave, layer resonance occurs at frequencies depending on the ratio of the wave velocity to the thickness of the layer [3, 4]. This phenomenon results in the local minima of the amplitude spectrum of the reflected wave from the layer due to destructive interference. In structures with multiple layers, the spectral characteristics of the elastic waves become more complicated.

While numerous studies have been carried out on the acoustic properties of layered structures so far, the effect of viscoelastic layers on wave propagation [5–9] is not fully revealed compared to purely elastic cases [10–16]. Viscoelastic materials transform the energy of sound waves into heat and attenuate the propagating waves. However, in the cases of layered structures, viscoelasticity sometimes facilitates wave resonances appearing in the reflection spectrum. Lavrentyev and Rokhlin [17] investigated the wave interaction with a single planar viscoelastic layer sandwiched by semi-infinite dissimilar materials. They showed theoretically that for plane wave incidence on the layer from the side of the semi-infinite material with lower acoustic impedance, the increase of the attenuation factor in the layer can make local minima of the amplitude of the reflection spectrum deep and narrow. The amplitude of the reflection spectrum at the layer resonance frequency becomes zero at a specific condition, called critical attenuation [17]. The critical attenuation condition for a single viscoelastic layer was analytically derived under several approximations.

To the authors' knowledge, however, the critical attenuation behavior has been reported only for the case of the single layer between semi-infinite dissimilar materials. Recently, Mori *et al.* [18] examined the wave propagation in a metal-plastic bilayer laminate placed in water theoretically and experimentally, showing that the damping property of the plastic layer contributes to the appearance of the layer resonance in the reflection spectrum. Nevertheless, the quantitative effect of the viscoelasticity on the resonance frequencies of the plastic layer has not been shown, and it remains unclear whether critical attenuation occurs in the bilayer laminates.

The present study aims to reveal the wave resonance and the critical attenuation behavior in metal-plastic bilayer laminates. Theoretical analysis is performed to derive the conditions of the layer resonance and the critical attenuation based on several approximations. The viscoelastic effects on the responses of the laminates to normal wave incidence are examined by comparing the exact and approximate results. Experimental results are shown to validate the theoretical findings and to investigate how the wave resonance and the critical attenuation appear.

This paper is structured as follows. In Section 2, the modeling of a bilayer elastic-viscoelastic laminate in an infinite medium is described. The loss factor is introduced when modeling the viscoelastic material, and the interaction of a normally incident wave with the laminate is formulated. Approximate formulae are obtained based on Taylor expansions with respect to the loss factor. In Section 3, the theoretical results are shown for two different cases, i.e. purely elastic and viscoelastic laminates. In Section 4, the results of the ultrasonic measurement are shown for two types of metal-plastic laminates and are used to discuss the theoretical results.

2. Theory

2.1 Modeling and formulation

As shown in Fig. 1(a), a bilayer laminate is placed in an infinite medium and is subjected to normal wave incidence. The medium surrounding the laminate, called medium 1, is lossless. The laminate consists of two planar homogeneous layers called layers 2 and 3 with thicknesses d_2 and d_3, respectively. The incident wave propagates along the x axis corresponding to the thickness direction. When a longitudinal plane wave is incident on the laminate from the side of layer 3, the wave propagation substantially becomes one-dimensional. In the frequency domain, the wave propagation behavior obeys

$$-\rho\omega^2 u = \frac{\partial \sigma}{\partial x}, \tag{1}$$

where ρ is the mass density of a medium, $\omega = 2\pi f$ is angular frequency, f is frequency, and $u(x, \omega)$ and $\sigma(x, \omega)$ are the frequency-domain representations of the displacement and normal stress components in the x direction. Harmonic wave components propagating in the x direction are represented by $\exp\{\mathrm{i}(kx-\omega t)\}$, where k is wavenumber, t is time, and $\mathrm{i} = \sqrt{-1}$.

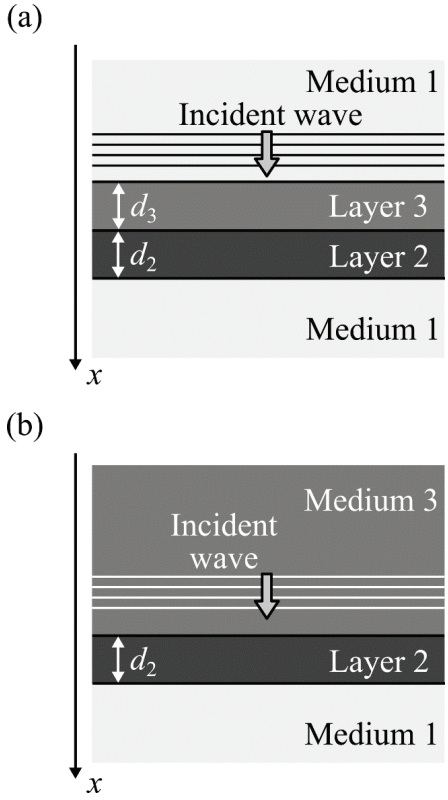

Fig. 1 Theoretical models of (a) a bilayer laminate in an infinite medium and (b) a bottom layer (layer 2) sandwiched by dissimilar media, subjected to normal wave incidence.

In this study, layers 3 and 2 are assumed to be plastic and metal, which are modeled as linear viscoelastic and purely elastic bodies, respectively. If the temperature variation by the wave attenuation in a linear viscoelastic material is negligible, its stress-strain relation can be modeled by [19–21]

$$\sigma = (E - \mathrm{i}D)\varepsilon = \rho c^2(1 - \mathrm{i}\zeta)\frac{\partial u}{\partial x}, \tag{2}$$

where $\varepsilon(x, \omega)$ is the frequency-domain representation of the normal strain, E–iD is complex elastic modulus ($D > 0$), $c = (E/\rho)^{1/2}$ is wave velocity, and $\zeta = D/E$ is loss factor. In purely elastic materials, the loss factor can be set as $\zeta = 0$. In general, the loss factors of viscoelastic materials depend on frequency, but ζ is assumed to be frequency-invariant in this study. The validity of this assumption is mentioned in Section 4. The minus sign in the complex elastic modulus is based on the time-dependent terms of $\exp(-\mathrm{i}\omega t)$. By substituting Eq. (2) to Eq. (1) and considering a solution of a plane wave $u = A\exp\{\mathrm{i}(kx - \omega t)\}$, where A is a non-zero constant, the complex wavenumber can be obtained as $k = \omega/v$, where

$$v = c\sqrt{1 - \mathrm{i}\zeta} \tag{3}$$

is called complex wave velocity in this study. Let the mass density, wavenumber, wave velocity, and complex wave velocity of layer j (j = 2, 3) be ρ_j, k_j, c_j, and v_j, respectively. The loss factors of layers 3 and 2 are set as $\zeta_3 = \zeta$ and $\zeta_2 = 0$, respectively, which mean that $v_2 = c_2$ holds. The mass density and wave velocity of medium 1 are expressed as ρ_1 and c_1 (= v_1), respectively.

For the incidence of a sinusoidal wave with angular frequency ω on the bilayer laminate, the reflection spectrum of the stress component is theoretically expressed as [1]

$$R_\mathrm{b} = \frac{Z_{321}^\mathrm{in} - z_1}{Z_{321}^\mathrm{in} + z_1}, \tag{4}$$

where $z_m = \rho_m v_m$ is the complex acoustic impedance of material m (m = 1, 2, 3),

$$\begin{aligned} Z_{321}^\mathrm{in} &= \frac{Z_{21}^\mathrm{in} - \mathrm{i}z_3 \tan\phi_3}{z_3 - \mathrm{i}Z_{21}^\mathrm{in} \tan\phi_3} z_3 , \\ Z_{21}^\mathrm{in} &= \frac{z_1 - \mathrm{i}z_2 \tan\phi_2}{z_2 - \mathrm{i}z_1 \tan\phi_2} z_2 \end{aligned} \tag{5}$$

are the effective acoustic impedances of two substructures, respectively, and $\phi_j = \omega d_j / v_j$ (j = 2, 3). For example, the quantity Z_{321}^in is based on the subsurface structure in Fig. 1(a), i.e. layers 3 and 2, and lower semi-infinite medium 1. Substitution of Eq. (5) into Eq. (4) leads to [18]

$$R_\mathrm{b} = \frac{r_{13} + r_{321} \exp(2\mathrm{i}\phi_3)}{1 + r_{13} r_{321} \exp(2\mathrm{i}\phi_3)}, \tag{6}$$

where

$$r_{mn} = \frac{z_n - z_m}{z_n + z_m} \tag{7}$$

is stress reflection coefficient at a boundary between materials m and n for normal wave incidence from material m (m, n = 1, 2, 3), and

$$r_{321} = \frac{Z_{21}^\mathrm{in} - z_3}{Z_{21}^\mathrm{in} + z_3} = \frac{r_{32} + r_{21} \exp(2\mathrm{i}\phi_2)}{1 + r_{32} r_{21} \exp(2\mathrm{i}\phi_2)} \tag{8}$$

corresponds to stress reflection spectrum for a single layer shown in Fig. 1(b), i.e. layer 2 sandwiched by semi-infinite media 3 and 1. It is noted that the reflection spectrum r_{321} depends on frequency, while the reflection coefficient r_{mn} is frequency-independent.

Due to the viscoelasticity of layer 3, the reflection coefficients r_{13} and r_{32} have non-zero imaginary parts. For example, the reflection coefficient r_{13} can be expressed as $r_{13} = |r_{13}|\exp(\mathrm{i}\theta_{13})$, where θ_{13} is real. When the reflection spectrum r_{321} in Eq. (8) is given as $r_{321} = |r_{321}|\exp(\mathrm{i}\theta_{321})$, Eq. (6) can be rewritten as

$$R_\mathrm{b} = \frac{|r_{13}| + |r_{321}| \exp(-2q) \exp[\mathrm{i}(2p + \theta_{321} - \theta_{13})]}{1 + |r_{13}||r_{321}| \exp(-2q) \exp[\mathrm{i}(2p + \theta_{13} + \theta_{321})]} \exp(\mathrm{i}\theta_{13}) , \tag{9}$$

where $p = \mathrm{Re}(\omega d_3/v_3)$, $q = \mathrm{Im}(\omega d_3/v_3)$, and θ_{321} is real.

2.2 Resonance and critical attenuation in bilayer laminates

The amplitude of the reflection spectrum $|R_b|$ is a function of frequency, and wave resonances are closely associated with the local minima of $|R_b|$. As mentioned in Ref. [17], the numerator of R_b in Eq. (9) plays a dominant role when the amplitude of the reflection spectrum $|R_b|$ takes a local minimum. When the acoustic impedance of layer 2 is higher than those of media 1 and 3, the amplitude of the reflection spectrum for layer 2 shown in Fig. 1(b), i.e. $|r_{321}|$, takes a local minimum at the angular frequency $\omega = \omega_{2,n}$ (n = 1, 2, …), where [4]

$$\omega_{2,n} = \frac{n\pi}{\tau_2} \tag{10}$$

and $\tau_2 = d_2/c_2$. If the frequency dependence of $\exp[i(2p+\theta_{321}-\theta_{13})]$ is sufficiently weak in the vicinity of $\omega = \omega_{2,n}$, $|R_b|$ has a local minimum due to the resonance of layer 2.

On the other hand, the frequency dependence of $|r_{321}|$ is expected to be relatively insignificant in the off-resonance of layer 2. In this case, the reflection spectrum $|R_b|$ takes a local minimum when the two terms in the numerator of Eq. (9) are in opposite phases [17]. Namely, the resonance in layer 3 occurs at the angular frequency $\omega = \omega_{3,m}$ (m = 1, 2, …) that satisfies

$$\omega_{3,m}\tau_3 \cdot \mathrm{Re}\left(\frac{1}{\sqrt{1-i\zeta}}\right) = \left(m-\frac{1}{2}\right)\pi + \frac{\theta_{13}-\theta_{321}}{2}, \tag{11}$$

where $\tau_3 = d_3/c_3$. Furthermore, the reflection spectrum at the mth-order resonance angular frequency $\omega = \omega_{3,m}$ is expected to become $R_b = 0$ if the loss factor satisfies $\zeta = \zeta_m$, such that

$$\mathrm{Im}\left(\frac{1}{\sqrt{1-i\zeta_m}}\right) = \frac{1}{2\omega_{3,m}\tau_3}\ln\frac{|r_{321}|}{|r_{13}|}. \tag{12}$$

By replacing $|r_{321}|$ for $|r_{32}|$ and assuming $\zeta_m \ll 1$, Eq. (12) is reduced to the critical attenuation condition for a viscoelastic layer between dissimilar semi-infinite materials given in Ref. [17]. Consequently, it is predicted that critical attenuation occurs not only in a single viscoelastic layer but also in the case of a bilayer laminate.

Equations (11) and (12) are nonlinear equations for the resonance angular frequency $\omega_{3,m}$ and the critical loss factor ζ_m, respectively, and cannot analytically be solved. In what follows, similarly to Ref. [17], Taylor expansion around the loss factor $\zeta = 0$ is employed to simplify the above conditions.

2.2.1 Conditions of resonance and critical attenuation: zeroth-order approximation

Under the zeroth-order approximation around the loss factor $\zeta = 0$, Eq. (11) gives the condition of the resonance in layer 3 as

$$\omega_{3,m}^{(0)}\tau_3 = \left(m-\frac{1}{2}\right)\pi + \frac{\theta_{13}^{(0)}-\theta_{321}^{(0)}}{2}, \tag{13}$$

where the superscript (0) represents the quantities at $\zeta = 0$. Namely, based on Eqs. (7) and (8),

$$\theta_{13}^{(0)} = \arg\left(r_{13}^{(0)}\right), \qquad \theta_{321}^{(0)} = \arg\left(r_{321}^{(0)}\right), \tag{14}$$

where

$$r_{13}^{(0)} = \frac{z_3^{(0)} - z_1}{z_3^{(0)} + z_1}, \qquad r_{321}^{(0)} = \frac{r_{32}^{(0)} + r_{21}\exp(2\mathrm{i}\phi_{2m})}{1 + r_{32}^{(0)} r_{21}\exp(2\mathrm{i}\phi_{2m})}, \tag{15}$$

$$r_{32}^{(0)} = \frac{z_2 - z_3^{(0)}}{z_2 + z_3^{(0)}} = \frac{1 - z_{32}}{1 + z_{32}}, \qquad r_{21} = \frac{z_1 - z_2}{z_1 + z_2} = -\frac{1 - z_{12}}{1 + z_{12}}, \tag{16}$$

$$z_3^{(0)} = \rho_3 c_3,\ z_{32} = z_3^{(0)}/z_2,\ z_{12} = z_1/z_2,\ \phi_{2m} = \omega_{3,m}^{(0)}\tau_2. \tag{17}$$

Since $r_{13}^{(0)}$ is real, $\theta_{13}^{(0)} = 0$ if $z_3^{(0)} > z_1$, and otherwise $\theta_{13}^{(0)} = \pi$. Substitution of Eqs. (16) and (17) into Eq. (15) leads to

$$r_{321}^{(0)} = \frac{(z_{12} - z_{32})\cos\phi_{2m} - \mathrm{i}(1 - z_{12}z_{32})\sin\phi_{2m}}{(z_{12} + z_{32})\cos\phi_{2m} - \mathrm{i}(1 + z_{12}z_{32})\sin\phi_{2m}}. \tag{18}$$

Thus,

$$\left|r_{321}^{(0)}\right| = \sqrt{\frac{(z_{12} - z_{32})^2\cos^2\phi_{2m} + (1 - z_{12}z_{32})^2\sin^2\phi_{2m}}{(z_{12} + z_{32})^2\cos^2\phi_{2m} + (1 + z_{12}z_{32})^2\sin^2\phi_{2m}}}, \tag{19}$$

$$\begin{aligned}\tan\theta_{321}^{(0)} &= -2z_{32}(1 - z_{12}^2)g(z_{12}, z_{32}),\\ g(z_{12}, z_{32}) &= \frac{\sin\phi_{2m}\cos\phi_{2m}}{(z_{12}^2 - z_{32}^2)\cos^2\phi_{2m} + (1 - z_{32}^2 z_{12}^2)\sin^2\phi_{2m}}.\end{aligned} \tag{20}$$

The function $g(z_{12}, z_{32})$ is expressed as Taylor expansion around $(z_{12}, z_{32}) = (0, 0)$, i.e.

$$g(z_{12}, z_{32}) = \frac{1}{\tan\phi_{2m}} + \frac{z_{12}^2}{2}\frac{\partial^2 g(0,0)}{\partial z_{12}^2} + \frac{z_{32}^2}{2}\frac{\partial^2 g(0,0)}{\partial z_{32}^2} + \cdots. \tag{21}$$

If the acoustic impedance of layer 2 is sufficiently higher than those of layer 3 and medium 1, i.e. $z_{12}, z_{32} \ll 1$, Eq. (20) can be simplified as

$$\tan\theta_{321}^{(0)} = -2z_{32}(1 - z_{12}^2)\left(\frac{1}{\tan\phi_{2m}} + \cdots\right) \cong -\frac{2z_{32}}{\tan\phi_{2m}} \equiv -A_m. \tag{22}$$

This leads to

$$\theta_{321}^{(0)} = -\tan^{-1}A_m. \tag{23}$$

As a result, the zeroth-order resonance condition of Eq. (13) is rewritten as

$$\omega_{3,m}^{(0)}\tau_3 = \left(m - \frac{1}{2}\right)\pi + \frac{\theta_{13}^{(0)}}{2} + \frac{1}{2}\tan^{-1}A_m, \tag{24}$$

which is an explicit form of a nonlinear equation with the resonance angular frequency $\omega_{3,m}^{(0)}$. If the third term in the right-hand side is negligible, Eq. (24) is reduced to

$$\omega_{3,m}^{(0)}\tau_3 = \left(m - \frac{1}{2}\right)\pi + \frac{\theta_{13}^{(0)}}{2}, \tag{25}$$

158 which corresponds to the resonance condition of a single layer [18]. Namely, $\tan^{-1}A_m$ in Eq. (24)
159 represents the coupling effect between layers 3 and 2.
160 The zeroth-order approximation of the resonance angular frequency is applied to the critical
161 attenuation condition of Eq. (12). If the critical loss factor for the *m*th-order resonance is assumed
162 to be sufficiently low, it can be expressed as

$$\zeta_m^{(0)} = \frac{1}{\omega_{3,m}^{(0)}\tau_3}\ln\frac{\left|r_{321}^{(0)}\right|}{\left|r_{13}^{(0)}\right|}. \tag{26}$$

163 If the coupling effect of layers 3 and 2 is weak, i.e. $|\tan\phi_{2m}| \gg 1$, Eq. (19) is simplified as

$$\left|r_{321}^{(0)}\right| \cong \left|\frac{1 - z_{12}z_{32}}{1 + z_{12}z_{32}}\right|, \tag{27}$$

164 leading to

$$\zeta_m^{(0)} = \frac{1}{\omega_{3,m}^{(0)}\tau_3}\ln\left|\frac{(1 - z_{12}z_{32})(z_{12} + z_{32})}{(1 + z_{12}z_{32})(z_{12} - z_{32})}\right|. \tag{28}$$

165 This formula gives the zeroth-order approximation of the critical loss factor if the corresponding
166 resonance frequency of layer 3 is already calculated.

167 *2.2.2 Second-order approximation of resonance condition*
168 The zeroth-order approximation of the resonance frequency in layer 3, given by Eq. (24), does
169 not provide the dependence on the loss factor ζ. In this section, the terms up to the second order
170 are taken into account. The *m*th-order resonance condition of Eq. (11) becomes

$$\omega_{3,m}^{(2)}\tau_3 = \left(1 + \frac{\zeta^2}{2}\right)\left[\left(m - \frac{1}{2}\right)\pi + \frac{\theta_{13}^{(2)} - \theta_{321}^{(2)}}{2}\right], \tag{29}$$

171 where the superscript (2) represents the second-order approximation around $\zeta = 0$. The reflection
172 coefficient r_{13} can be expanded as

$$\begin{aligned} r_{13}^{(2)} &= r_{13}^{(0)} + \zeta\left.\frac{\mathrm{d}r_{13}}{\mathrm{d}\zeta}\right|_{\zeta=0} + \frac{\zeta^2}{2}\left.\frac{\mathrm{d}^2 r_{13}}{\mathrm{d}\zeta^2}\right|_{\zeta=0} \\ &= r_{13}^{(0)}\left[1 + \frac{\zeta^2}{16}\left(\frac{1}{r_{13}^{(0)}} - r_{13}^{(0)}\right)\left(3 - t_{13}^{(0)}\right) - \mathrm{i}\frac{\zeta}{4}\left(\frac{1}{r_{13}^{(0)}} - r_{13}^{(0)}\right)\right], \end{aligned} \tag{30}$$

173 where $t_{13}^{(0)} = 2z_1/(z_3^{(0)}+z_1)$, and its phase is obtained as

$$\theta_{13}^{(2)} = \theta_{13}^{(0)} + \arg\left[1 + \frac{\zeta^2}{16}\left(\frac{1}{r_{13}^{(0)}} - r_{13}^{(0)}\right)\left(3 - t_{13}^{(0)}\right) - \mathrm{i}\frac{\zeta}{4}\left(\frac{1}{r_{13}^{(0)}} - r_{13}^{(0)}\right)\right]. \tag{31}$$

174 Similar expansion is performed on the reflection spectrum r_{321}. Since

$$
\begin{aligned}
r_{321}^{(2)} &= r_{321}^{(0)} + \zeta \left.\frac{\mathrm{d}r_{321}}{\mathrm{d}\zeta}\right|_{\zeta=0} + \frac{\zeta^2}{2}\left.\frac{\mathrm{d}^2 r_{321}}{\mathrm{d}\zeta^2}\right|_{\zeta=0} \\
&= r_{321}^{(0)}\left[1 - \frac{\zeta^2}{16}\left(\frac{1}{r_{321}^{(0)}} - r_{321}^{(0)}\right)\left(3 - t_{321}^{(0)}\right) + \mathrm{i}\frac{\zeta}{4}\left(\frac{1}{r_{321}^{(0)}} - r_{321}^{(0)}\right)\right],
\end{aligned}
\tag{32}
$$

where $t_{321}^{(0)} = 2z_{21}^{\mathrm{in}}/(z_3^{(0)}+z_{21}^{\mathrm{in}})$, its phase is expressed by

$$
\theta_{321}^{(2)} = \theta_{321}^{(0)} + \arg\left[1 - \frac{\zeta^2}{16}\left(\frac{1}{r_{321}^{(0)}} - r_{321}^{(0)}\right)\left(3 - t_{321}^{(0)}\right) + \mathrm{i}\frac{\zeta}{4}\left(\frac{1}{r_{321}^{(0)}} - r_{321}^{(0)}\right)\right]. \tag{33}
$$

Substitution of Eqs. (31) and (33) into Eq. (29) leads to

$$
\omega_{3,m}^{(2)}\tau_3 = \left(1 + \frac{\zeta^2}{2}\right)\left(\omega_{3,m}^{(0)}\tau_3 + \frac{\Phi_{13}^{(2)} - \Phi_{321}^{(2)}}{2}\right). \tag{34}
$$

where

$$
\begin{aligned}
\Phi_{13}^{(2)} &= \arg\left[1 + \frac{\zeta^2}{16}\left(\frac{1}{r_{13}^{(0)}} - r_{13}^{(0)}\right)\left(3 - t_{13}^{(0)}\right) - \mathrm{i}\frac{\zeta}{4}\left(\frac{1}{r_{13}^{(0)}} - r_{13}^{(0)}\right)\right], \\
\Phi_{321}^{(2)} &= \arg\left[1 - \frac{\zeta^2}{16}\left(\frac{1}{r_{321}^{(0)}} - r_{321}^{(0)}\right)\left(3 - t_{321}^{(0)}\right) + \mathrm{i}\frac{\zeta}{4}\left(\frac{1}{r_{321}^{(0)}} - r_{321}^{(0)}\right)\right].
\end{aligned}
\tag{35}
$$

When more than third-order terms with respect to the loss factor are neglected, Eq. (34) becomes

$$
\omega_{3,m}^{(2)}\tau_3 = \omega_{3,m}^{(0)}\tau_3 + \zeta\chi_1 + \frac{\zeta^2}{2}\omega_{3,m}^{(0)}\tau_3, \tag{36}
$$

where

$$
\chi_1 = -\frac{1}{8}\left\{\frac{1}{r_{13}^{(0)}} - r_{13}^{(0)} + \left(\frac{1}{\left|r_{321}^{(0)}\right|} - \left|r_{321}^{(0)}\right|\right)\cos\theta_{321}^{(0)}\right\}. \tag{37}
$$

If $\left|\theta_{321}^{(0)}\right| \ll 1$ holds, it is further simplified as

$$
\chi_1 \cong -\frac{1}{8}\left(r_{13}^{(0)} + \left|r_{321}^{(0)}\right|\right)\left(\frac{1}{r_{13}^{(0)}\left|r_{321}^{(0)}\right|} - 1\right). \tag{38}
$$

If $z_3^{(0)} > z_1$, the zeroth-order reflection coefficient $r_{13}^{(0)}$ satisfies $0 < r_{13}^{(0)} < 1$. Since $0 < \left|r_{321}^{(0)}\right| < 1$, the coefficient χ_1 becomes $\chi_1 < 0$. On the other hand, the second-order term in the right-hand side of Eq. (36) is always positive.

3. Theoretical results

3.1 Case of purely elastic laminates

Before considering viscoelastic cases, the responses of purely elastic bilayer laminates are investigated in this section. Layer 2 is modeled by an elastic layer of thickness $d_2 = 2$ mm, mass density $\rho_2 = 2.65 \times 10^3$ kg/m^3, and wave velocity $c_2 = 6.41$ km/s, which are based on the properties

of aluminum alloy 5052. The surrounding medium is assumed to be water with $\rho_1 = 1.00 \times 10^3$ kg/m^3 and $c_1 = 1.48$ km/s. In this case, the acoustic impedance ratio z_{12} is $z_{12} = 0.0871$. At $\zeta = 0$, the reflection spectrum for the bilayer laminate is calculated for different acoustic impedance ratios z_{32} and normalized quantities $\tau_{32} = \tau_3/\tau_2$. In this study, τ_{32} is called the normalized thickness ratio. If layer 3 is polystyrene of thickness $d_3 = 1.2$ mm, mass density $\rho_3 = 1.02 \times 10^3$ kg/m^3, and wave velocity $c_3 = 2.16$ km/s, the above quantities are obtained as $z_{32} = 0.130$ and $\tau_{32} = 1.78$.

Fig. 2(a) shows the amplitudes of the reflection spectrum as functions of frequency, obtained by Eq. (6) at a fixed normalized thickness ratio $\tau_{32} = 1.5$. When the acoustic impedance ratio is low, i.e. $z_{32} = 0.1$, local minima lower than 0.2 appear periodically at 1.602 MHz, 3.204 MHz, 4.808 MHz, etc. These drops result from the resonance in layer 2, and the resonance frequencies are in good agreement with Eq. (10). However, at the higher acoustic impedance ratio, i.e. $z_{32} = 0.3$, additional local minima emerge. Namely, if the acoustic impedance of layer 3 is closer to that of layer 2, the effect of layer 3 on the reflection spectrum becomes more significant. This feature is further examined later.

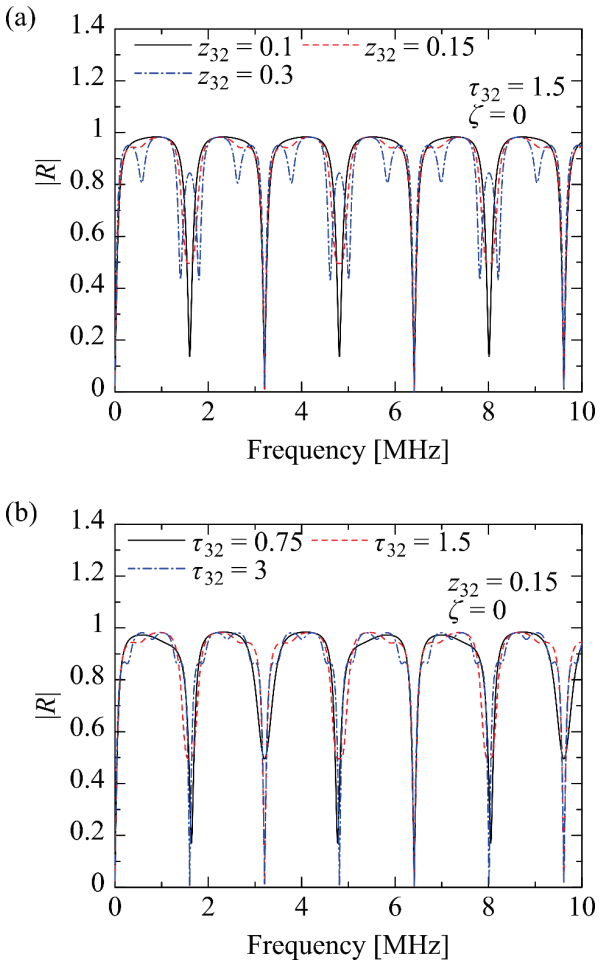

Fig. 2 Amplitudes of the reflection spectrum for purely elastic laminates calculated for (a) different acoustic impedance ratios z_{32} at $\tau_{32} = 1.5$ and (b) different normalized thickness ratios τ_{32} at $z_{32} = 0.15$.

Fig. 2(b) shows the amplitudes of the reflection spectrum calculated by Eq. (6) for different normalized thickness ratios τ_{32} at a fixed acoustic impedance ratio $z_{32} = 0.15$. In this figure, local minima resulting from the resonance in layer 2, which have also been confirmed in Fig. 2(a), are clear if the normalized thickness ratio τ_{32} changes. The normalized thickness ratio τ_{32} seems to affect the reflection spectra, particularly in the vicinity of the local maxima.

The frequencies at which local minima appear were extracted below 10 MHz from the amplitudes of the reflection spectrum calculated by Eq. (6) in various conditions. Fig. 3(a) and (b) show the local minimum frequencies as functions of the acoustic impedance ratio z_{32} and the normalized thickness ratio τ_{32}, respectively. In Fig. 3(a), the normalized thickness ratio is fixed at $\tau_{32} = 1.5$, and in Fig. 3(b), the acoustic impedance ratio is set as $z_{32} = 0.15$. It is found that the variation of the resonance frequencies is almost flat in Fig. 3(a), but some of the resonance frequencies decrease significantly with increasing normalized thickness ratio τ_{32} in Fig. 3(b).

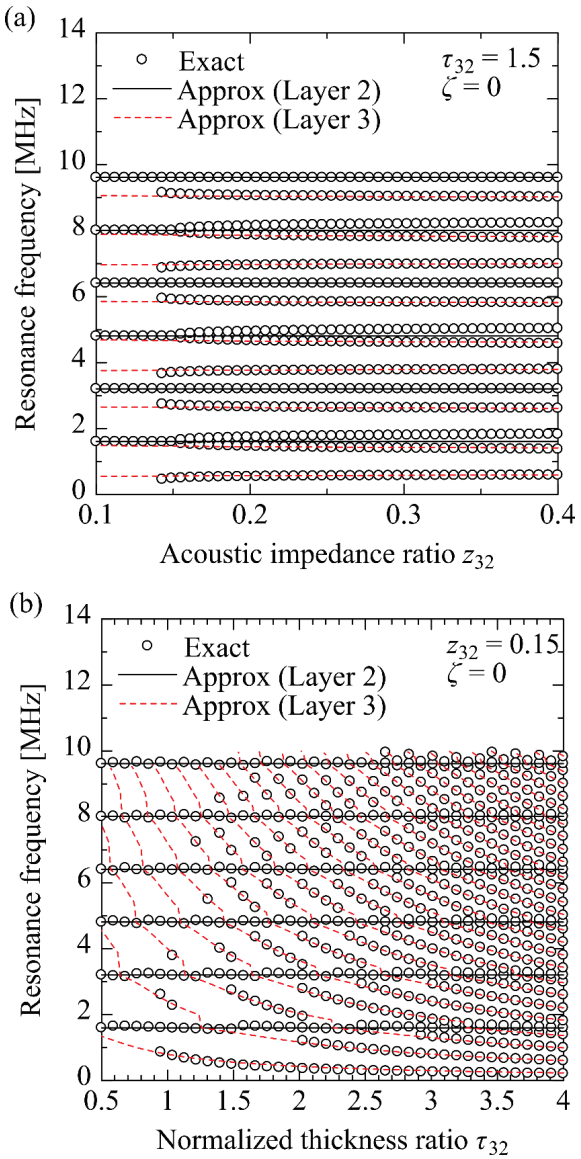

Fig. 3 Relations of the local minimum frequencies to (a) the acoustic impedance ratio z_{32} at τ_{32} = 1.5 and (b) the normalized thickness ratio τ_{32} at z_{32} = 0.15 extracted from the amplitudes of the reflection spectrum calculated by Eq. (6) for purely elastic laminates, together with the zeroth-order approximate results for the resonance frequencies of layers 2 and 3.

For comparison, the zeroth-order approximation results for the resonance frequencies of layers 2 and 3 were obtained by Eqs. (10) and (24), respectively. The nonlinear equation of Eq. (24) was numerically solved with the bisection method. The obtained results are shown together in Fig. 3(a) and (b). On the whole, the exact values of the resonance frequencies are in good agreement with the approximate results. In particular, the approximate results in Fig. 3(b) fairly reproduce that the resonance frequencies of layer 2 are almost unchanged if the normalized thickness ratio τ_{32} varies, while those of layer 3 decrease with decreasing τ_{32}.

It is noted that the approximate results for the resonance frequencies of layer 2, given by Eq. (10), do not depend on the acoustic impedance ratio z_{32}. In Fig. 3(a), however, if the approximate result for a resonance frequency of layer 2 is close to that for layer 3, the exact result for the resonance frequency of layer 2 tends to increase as the acoustic impedance ratio z_{32} increases. For example, the resonance frequency of 1.603 MHz at $z_{32} = 0.1$ becomes 1.831 MHz at $z_{32} = 0.4$. This deviation is probably attributed to the fact that the coupling effects between layers 2 and 3 are neglected in the approximate formula of Eq. (10). The modification of Eq. (10) could lead to better agreement between the exact and approximate results for the resonance frequencies of layer 2. However, this is not further explored because the present study has an interest in the resonance phenomenon occurring in layer 3.

In Fig. 3(a), the resonance frequencies of layer 3 are well reproduced by the approximate results if the acoustic impedance ratio z_{32} increases. This can be attributed to the coupling term in Eq. (24). On the other hand, in $z_{32} < 0.14$, the exact results for the resonance frequencies of layer 3 could not be obtained because the local minima do not appear in the amplitude of the reflection spectrum. This phenomenon corresponds to the result in Ref. [18] that the amplitude spectrum of the reflected wave from a purely elastic bilayer laminate is not affected by the resonance of the layer with lower acoustic impedance. The resonance effect is expected to emerge if the loss factor of layer 3 is non-zero [18]. In the next section, the effect of the loss factor ζ of layer 3 on the reflection spectrum is examined.

3.2 Case of viscoelastic laminates

The amplitudes of the reflection spectrum for viscoelastic-elastic bilayer laminates were calculated by Eq. (6). Based on the measured result for polystyrene, the loss factor was set to be $\zeta = 0.02$. Fig. 4(a) and (b) show the obtained results for different acoustic impedance ratios z_{32} and normalized thickness ratios τ_{32}, respectively. The parameters except for the loss factor ζ in Fig. 4(a) and (b) are the same as those in Fig. 2(a) and (b), respectively. In Fig. 2(a), only local minima corresponding to the resonance of layer 2 have appeared at $z_{32} = 0.1$. However, in Fig. 4(a), the reflection spectrum has additional local minima at $z_{32} = 0.1$ when $\zeta = 0.02$. This result implies that the effect of the non-zero loss factor ζ deepens the local minima of the reflection spectrum due to the resonance of layer 3. The additional local minimum frequencies appear to be unchanged at the high acoustic impedance ratio $z_{32} = 0.3$. In Fig. 4(b), the normalized thickness ratio τ_{32} affects the intervals of local minima in the reflection spectrum. This trend is different from the case of $\zeta = 0$ in which only clear local minima corresponding to the resonance of layer 2 appear even if the normalized thickness ratio τ_{32} changes, as shown in Fig. 2(b). In what follows, the characteristics of the resonance and critical attenuation are separately investigated.

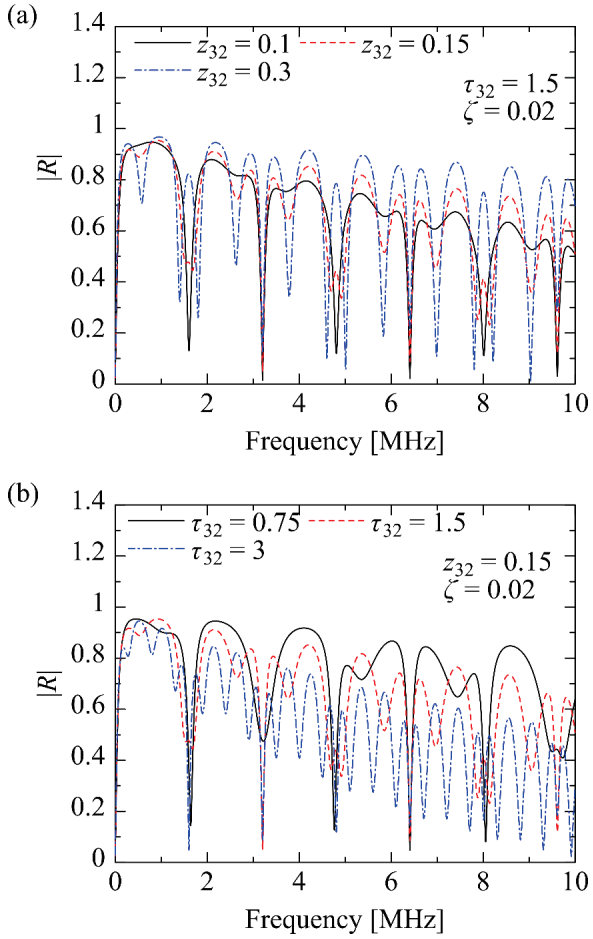

Fig. 4 Amplitudes of the reflection spectrum for viscoelastic-elastic bilayer laminates of $\zeta = 0.02$, calculated for (a) different acoustic impedance ratios z_{32} at $\tau_{32} = 1.5$ and (b) different normalized thickness ratios τ_{32} at $z_{32} = 0.15$.

3.2.1 Resonance behavior

The resonance frequencies lower than 10 MHz were extracted from the reflection spectrum calculated by Eq. (6) for viscoelastic laminates of the loss factor $\zeta = 0.02$. The obtained results are shown as the functions of the acoustic impedance ratio z_{32} and the normalized thickness ratio τ_{32} in Fig. 5(a) and (b), respectively. In Fig. 5(a), the normalized thickness ratio is fixed at $\tau_{32} = 1.5$, and in Fig. 5(b), the acoustic impedance ratio is set as $z_{32} = 0.15$. For comparison, the second-order approximation of the resonance frequencies of layer 3 is calculated by Eqs. (36) and (37) and is shown in Fig. 5(a), together with the zeroth-order resonance frequencies obtained by Eqs. (10) and (24). It is found in Fig. 5(a) that the differences between the second- and zeroth-order approximate results are trivial. This fact is attributed to the sufficiently low loss factor $\zeta = 0.02$. Accordingly, only the zeroth-order approximate results are shown in Fig. 5(b) for comparison.

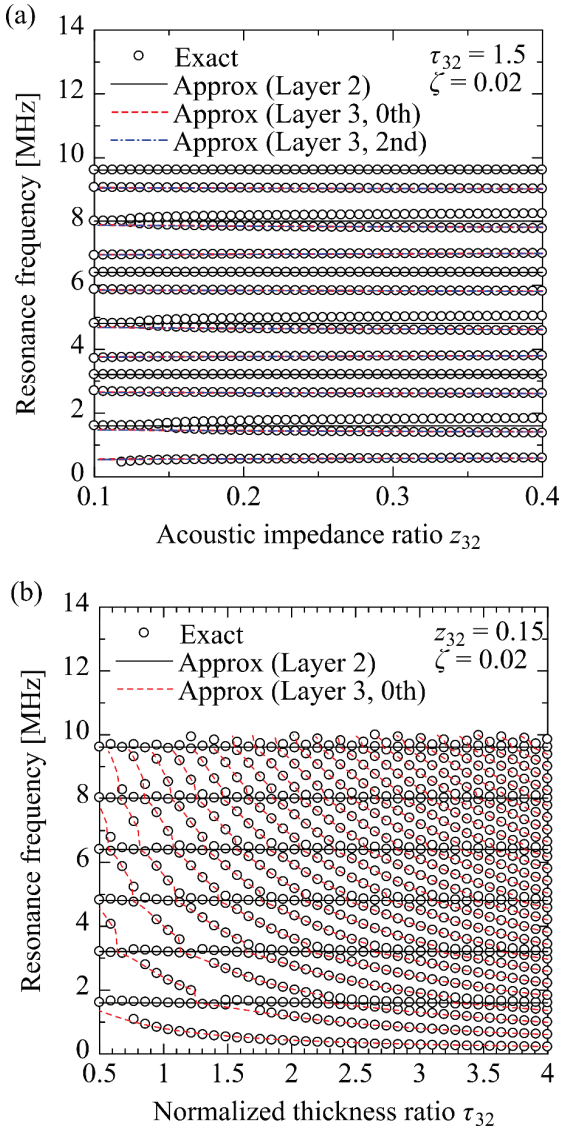

Fig. 5 Relations of the local minimum frequencies to (a) the acoustic impedance ratio z_{32} at τ_{32} = 1.5 and (b) the normalized thickness ratio τ_{32} at z_{32} = 0.15, extracted from the amplitudes of the reflection spectrum calculated by Eq. (6) for viscoelastic laminates of ζ = 0.02, together with the approximate results for the resonance frequencies of layers 2 and 3.

The exact resonance frequencies in Fig. 5(a) and (b) are fairly reproduced by the zeroth-order approximation for layers 2 and 3. This tendency is analogous to the cases of purely elastic laminates in Fig. 3(a) and (b). However, the exact results in Fig. 5(a) and (b) have more numbers of resonance frequencies of layer 3 than those in Fig. 3(a) and (b). For example, in Fig. 3(a), the exact values of the resonance frequencies of layer 3 are missing in $z_{32} < 0.14$ when $\zeta = 0$, but they appear when $\zeta = 0.02$ in Fig. 5(a). This difference results from the viscoelastic effect of layer 3 [18].

To clarify the quantitative effect of the loss factor ζ, the amplitudes of the reflection spectrum for the bilayer laminates were calculated for different loss factors by Eq. (6). Fig. 6 shows the obtained results at fixed acoustic impedance ratio $z_{32} = 0.15$ and normalized thickness ratio $\tau_{32} = 1.5$. At the resonance frequencies of layer 3 located below 6 MHz, e.g. 2.64 MHz and 3.76 MHz, the amplitude of the reflection spectrum decreases with increasing loss factor in $\zeta < 0.1$. Namely, the loss factor contributes to the generation of the local minima. However, this tendency is not confirmed at higher frequencies. For example, when $\zeta = 0.04$, the amplitude of the reflection spectrum at the resonance frequency of 9.06 MHz is smaller than that for $\zeta = 0.1$.

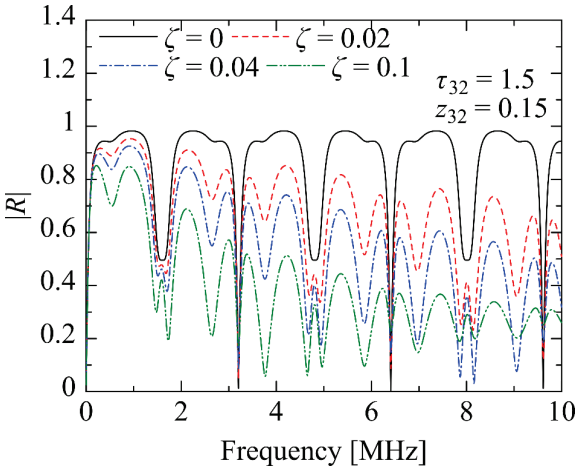

Fig. 6 Amplitudes of the reflection spectrum for viscoelastic laminates calculated for different loss factors ζ at fixed acoustic impedance ratio $z_{32} = 0.15$ and normalized thickness ratio $\tau_{32} = 1.5$.

The resonance frequencies were extracted from the reflection spectra calculated for different loss factors ζ at $z_{32} = 0.15$ and $\tau_{32} = 1.5$. Fig. 7 shows the results only for the resonance frequencies of layer 3 as functions of the loss factor in $\zeta < 0.3$. The frequency range was set to be down to 6 MHz to show the dependence on the loss factor more clearly. It is found in this figure that the effect of the loss factor ζ on the resonance frequencies is not significant, but some of the resonance frequencies slightly increase with increasing loss factor. For example, the resonance frequency 5.86 MHz at $\zeta = 0.006$ becomes 5.96 MHz at $\zeta = 0.3$. The resonance frequencies in the vicinity of 1.46 MHz and 4.67 MHz slightly decrease in $\zeta < 0.05$, but this behavior appears probably because the resonance frequencies of layer 2 exist nearby, as shown in Fig. 5(a). The coupling effect of layers 2 and 3 would be significant in these cases.

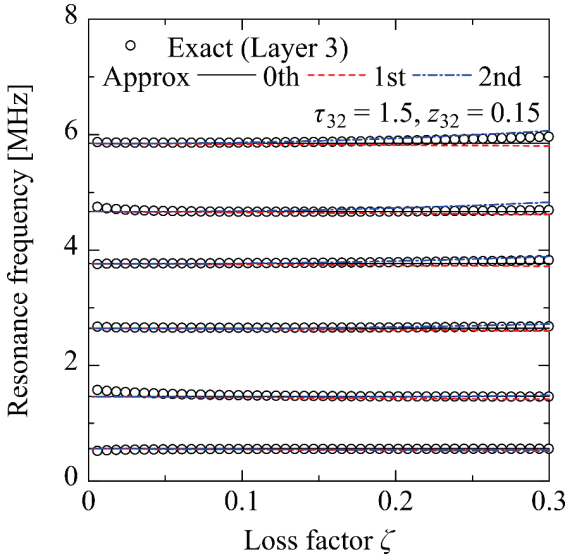

Fig. 7 Relations of the resonance frequencies of layer 3 to the loss factor ζ at fixed acoustic impedance ratio z_{32} = 0.15 and normalized thickness ratio τ_{32} = 1.5, extracted from the amplitudes of the reflection spectra calculated by Eq. (6), together with the approximate results.

The approximate results for the resonance frequencies of layer 3 with three different orders are shown together in Fig. 7. The zeroth-order resonance frequencies are invariant with the loss factor ζ. The resonance frequencies under the first-order approximation, obtained by eliminating the second-order term in Eq. (36), linearly decrease with increasing loss factor because the coefficient χ_1 is negative in this case. Consequently, the second-order term is necessary to reproduce the increasing behavior of the resonance frequencies with increasing loss factor in $\zeta <$ 0.3. However, the loss factor of common plastics is lower than $\zeta = 0.1$, implying that the higher-order terms do not play an apparent role. In other words, the zeroth-order approximation seems to be sufficient in predicting the resonance frequencies of a common plastic layer.

3.2.2 Critical attenuation behavior

The amplitudes of the reflection spectrum at the mth-order resonance of layer 3, denoted as $|R_{vm}|$ (m = 1, 2, …), are further examined in this section. Based on the results in the previous section, $|R_{vm}|$ was calculated as the amplitude of the reflection spectrum at the zeroth-order resonance angular frequency of layer 3, $\omega = \omega_{3,m}^{(0)}$, which is given by Eq. (24). Following Fig. 7, the amplitudes $|R_{vm}|$ for m = 1–6 are shown in Fig. 8 as the functions of the loss factor in $\zeta < 0.3$. The acoustic impedance ratio z_{32} and the normalized thickness ratio τ_{32} in Fig. 8 are the same as those in Fig. 7. It is shown in Fig. 8 that the amplitudes $|R_{vm}|$ at the second- to sixth-order resonances (m = 2–6) have deep minima at different loss factors. This phenomenon corresponds to critical attenuation in bilayer laminates.

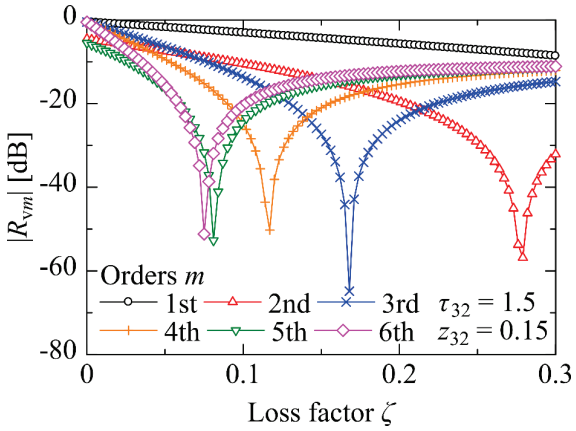

Fig. 8 Relations of the amplitudes of the reflection spectrum at different-order resonance frequencies of layer 3 to the loss factor ζ at fixed acoustic impedance ratio $z_{32} = 0.15$ and normalized thickness ratio $\tau_{32} = 1.5$, calculated by Eq. (6).

The variation of the amplitude $|R_{vm}|$ with the loss factor ζ was calculated for each order m, and the critical loss factor $\zeta = \zeta_m$ which minimizes $|R_{vm}|$ was sought in a range of $0.01 < \zeta < 1$. The obtained results are plotted with the resonance orders m = 1–15 in Fig. 9. The critical loss factor ζ_m decreases as the resonance order m increases. Larger loss factors would be necessary to realize the critical attenuation at low resonance frequencies.

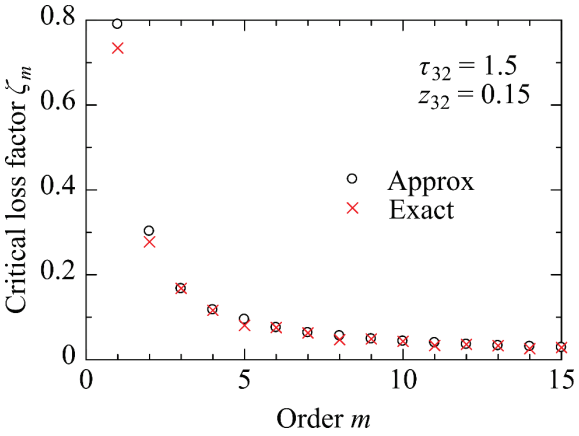

Fig. 9 Critical loss factors for different resonance orders extracted from the amplitudes of the reflection spectrum at fixed acoustic impedance ratio $z_{32} = 0.15$ and normalized thickness ratio $\tau_{32} = 1.5$, together with the zeroth-order approximate results based on Eq. (28).

Furthermore, the zeroth-order approximate results of the critical loss factor $\zeta_m^{(0)}$, calculated by Eq. (28), are shown together in Fig. 9. As a result, the zeroth-order results agree well with the exact critical loss factors. Namely, the decrease of the critical loss factor ζ_m with increasing resonance order m is well reproduced by the inverse proportion to the resonance angular frequency, as expressed in Eq. (28). In Fig. 9, the deviation between the exact and approximate results is

relatively distinct at low resonance orders probably because the loss factor is not sufficiently small to satisfy the zeroth-order approximation. The agreement might become better if higher-order terms are considered in the formula of the critical loss factor. However, in a practical sense, this extension could not be that essential because the loss factors of common plastics are not so high as $\zeta = 0.1$. The modification of the formula is not further explored in this study.

4. Experimental validation

4.1 Specimens and measurement setup

Ultrasonic measurements were performed on metal-plastic bonded specimens to examine and discuss the theoretical findings. The details of the specimens used in the experiments are summarized in Table 1. PS1.2/AL2.0 is a bonded specimen of polystyrene (PS) and aluminum alloy (AL) plates with thicknesses of 1.2 mm and 2.0 mm, respectively [18]. A cyanoacrylate adhesive (Henkel, Loctite 406) was used to join the two plates. Microscopic observation of side faces showed that PS1.2/AL2.0 had an adhesive layer with a thickness of 5.1 μm. PC1.5/AL0.8 corresponds to a bonded specimen of polycarbonate (PC) and AL plates with thicknesses of 1.55 mm and 0.8 mm, respectively, which was produced in a similar manner to PS1.2/AL2.0. The PS and PC sheets have square shapes with side lengths of 30 mm.

Table 1 Specimens used in the experiments.

Specimen	Description
PS1.2/AL2.0	Bonded specimen of 1.20 mm thick polystyrene plate and 2.00 mm thick aluminum alloy A5052 plate [18]
PC1.5/AL0.8	Bonded specimen of 1.55 mm thick polycarbonate plate and 0.80 mm thick aluminum A1050 plate
PS1.2	Polystyrene plate with a thickness of 1.20 mm
PC1.5	Polycarbonate plate with a thickness of 1.55 mm

The same experimental setup as Ref. [18] was used in the present study. The measurement was performed at room temperature, i.e. approximately 28 ℃. A specimen was placed in a water tank and subjected to normal wave incidence. An Olympus immersion transducer V311-SU with an element diameter of 0.5 inches and a nominal frequency of 10 MHz was used to emit the incident wave and detect the reflected waves from the specimen. The distance between the transducer and the specimen was approximately 20 mm. A spike pulse voltage was supplied to the transducer by a JSR Ultrasonics pulser/receiver DPR300. The reflection waveform was passed in a lowpass filter of 22.5 MHz and was recorded by a Tektronix oscilloscope MDO3014 after

averaging over 64 synchronized signals. The measured data were transferred to a PC via LabVIEW.

The measured waveform was analyzed by fast Fourier transform (FFT) to obtain its spectrum $P_L(f)$, where f is frequency. The reflection spectrum

$$R(f) = \frac{P_L(f)}{I(f)}, \tag{39}$$

was calculated, where $I(f)$ is the spectrum of the incident wave. The incident spectrum $I(f)$ was obtained based on the surface reflection waveform from a known material. In this study, a 10 mm thick stainless steel 303 block was used to measure the spectrum of the surface reflection waveform $P_S(f)$. The spectrum of the incident wave $I(f)$ was calculated by $I(f) = P_S(f)/r_{ws}$, where $r_{ws} = 0.938$ was the reflection coefficient between water and stainless steel obtained by Eq. (7) and the acoustic impedances of the two materials.

4.2 Experimental results and discussions

The measurements were first performed on single plastic and metal plates to obtain their material properties. Fig. 10(a) shows the amplitude of the reflection spectrum $|R|$ measured for a 1.55 mm thick PC plate, called PC1.5, in a frequency range of 6–11 MHz. It is noted that the measured reflection spectrum is shown in dB scales. This result was compared to the theoretical curve obtained by Eq. (8). The wave velocity c_{PC} and loss factor ζ_{PC} that reproduce the measured reflection spectrum were sought in a range of 2 km/s < c_{PC} < 3 km/s with an increment of 0.01 km/s and 0 < ζ_{PC} < 0.08 with an increment of 0.001. As a result, c_{PC} = 2.28 km/s and ζ_{PC} = 0.042 were obtained as optimal values for PC. The theoretical reflection spectrum calculated with these quantities is shown together in Fig. 10(a). It is found in this figure that the measured data are well reproduced by the theoretical reflection spectrum calculated with the estimated properties. This agreement implies that it is consistent to assume the frequency invariance regarding the loss factor of PC. Similar measurements were performed on a polystyrene plate of thickness 1.20 mm, called PS1.2, and two aluminum plates. The properties of each material were identified based on the measured spectra, as summarized in Table 2. The mass densities of the specimens were obtained by measuring the weights and dimensions. The material properties given in Table 2 are used when comparing the experimental data for the metal-plastic bonded specimens to the theoretical predictions.

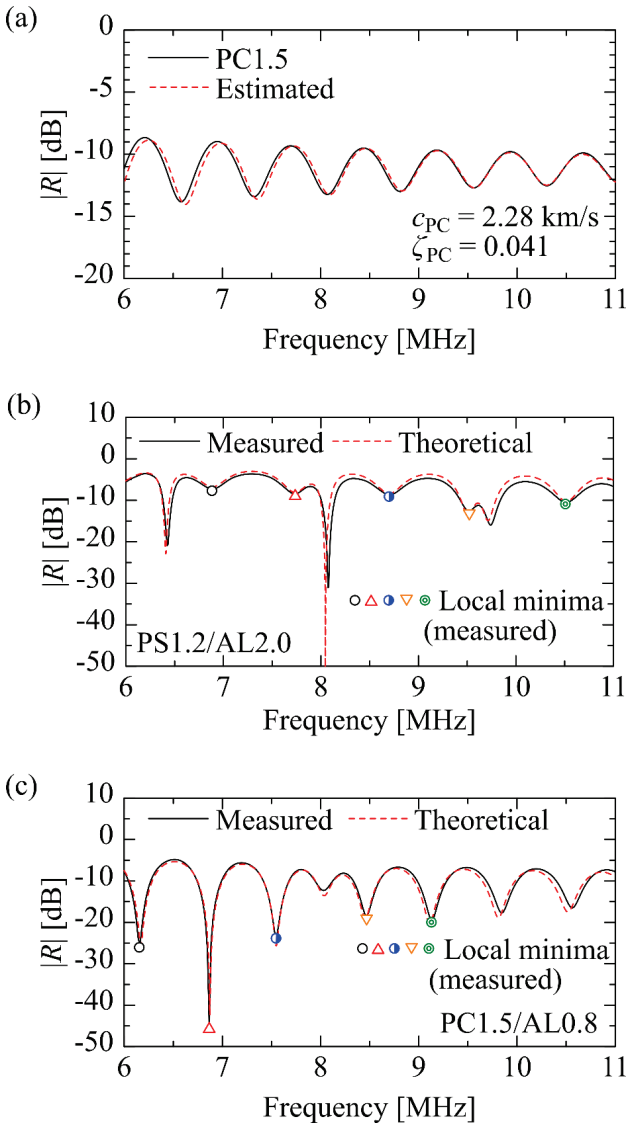

Fig. 10 Amplitudes of the reflection spectra measured for (a) PC1.5, (b) PS1.2/AL2.0, and (c) PC1.5/AL0.8, together with the corresponding theoretical curves. Some of the measured local minima at the resonance of the plastic layers are shown by symbols in (b) and (c).

Table 2 Material properties identified by ultrasonic measurements.

	c [km/s]	ζ	ρ [kg/m^3]
Polycarbonate (PC)	2.28	0.041	1.15×10^3
Polystyrene (PS)	2.16	0.020	1.02×10^3
Aluminum alloy 5052	6.41	0	2.65×10^3
Aluminum 1050	6.46	0	2.65×10^3

Fig. 10(b) and (c) show the amplitudes of the reflection spectra measured for the two bonded specimens, PS1.2/AL2.0 and PC1.5/AL0.8, respectively. The measured data for PS1.2/AL2.0 in Fig. 10(b) are based on Ref. [18]. It is found that local minima appear in the reflection spectra for both PS1.2/AL2.0 and PC1.5/AL0.8. The theoretical reflection spectrum was calculated for each specimen by Eq. (6) based on the material properties in Table 2. The obtained results when the thicknesses of the PS and PC layers are set to be 1.20 mm and 1.57 mm, respectively, are shown in Fig. 10(b) and (c), respectively. The experimental results are fairly reproduced by the theoretical curves. This agreement implies that the theoretical formulation regarding the reflection spectrum is sufficiently valid to reproduce the responses of the PS/AL and PC/AL laminates to normal wave incidence. Namely, the adhesive layers of the two specimens are sufficiently thin that they can be modeled as bilayer laminates.

In Section 3.2, the amplitudes of the reflection spectrum at the resonance of layer 3 (surface layer), i.e. $|R_{vm}|$, were theoretically examined for different loss factors ζ. However, it was difficult to change the loss factor continuously in the present experiment. Thus, the amplitudes $|R_v|$ for different resonance orders were investigated for the two specimens. In each case, five of the measured amplitudes at the resonance frequencies of the plastic layer were extracted, as represented by symbols in Fig. 10(b) and (c). The local minima at around 6.4 MHz and 8 MHz in Fig. 10(b) and 8 MHz in Fig. 10(c) correspond to the resonances of the AL layers, which are not considered here.

The obtained amplitudes $|R_v|$ for PS1.2/AL2.0 and PC1.5/AL0.8 are plotted in Fig. 11(a) and (b), respectively. The loss factors of the plastic layers in PS1.2/AL2.0 and PC1.5/AL0.8 are assumed to be $\zeta = 0.020$ and $\zeta = 0.041$, respectively, based on Table 2. The types of symbols in Fig. 11(a) and (b) are identical to those in Fig. 10(b) and (c), respectively. The theoretical relations of $|R_v|$ at the corresponding resonance orders to the loss factor ζ are shown together in Fig. 11(a) and (b). In the theoretical calculation, the zeroth-order approximate resonance frequencies were used to obtain the amplitudes. The colors of the lines and symbols in the figures correspond to the orders of the resonance. Fig. 11(a) and (b) show that the measured amplitudes $|R_v|$ are located almost on the theoretical curves. For PS1.2/AL2.0 in Fig. 11(a), the loss factor is much lower than the critical attenuation conditions in $\zeta > 0.04$. On the other hand, the experimental results for PC1.5/AL0.8 in Fig. 11(b) demonstrate that the amplitude represented by a red triangle almost satisfies the theoretical condition of the critical attenuation ($\zeta_m = 0.0418$). The amplitude at this resonance order would be sensitive to the loss factor in the vicinity of $\zeta = 0.0418$. The critical loss factors of the other orders in Fig. 11(b) are predicted to be in $0.025 < \zeta < 0.05$.

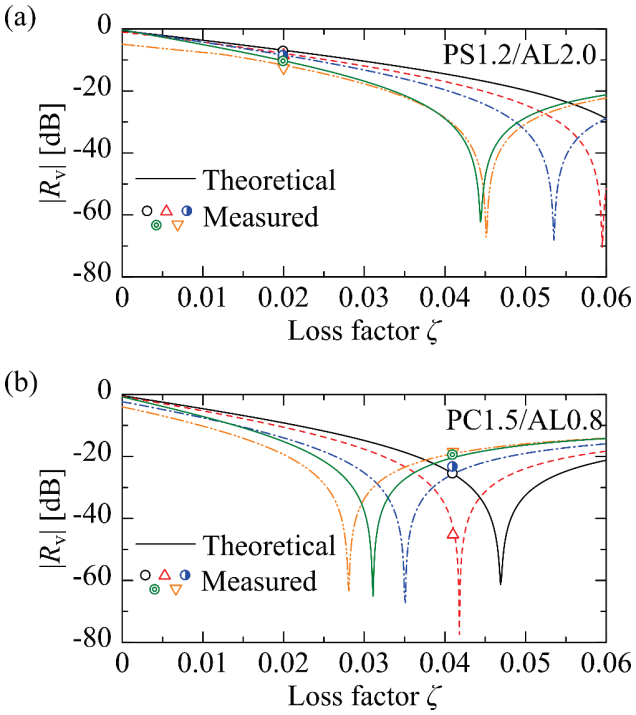

Fig. 11 Theoretical relations of the amplitudes $|R_v|$ at five different resonance orders for (a) PS1.2/AL2.0 and (b) PC1.5/AL0.8 to the loss factor ζ, and their comparison to the measured results. The experimental results correspond to the symbols shown in Fig. 10(a) and (b), and the colors of the lines and symbols represent the orders of the resonance. (For interpretation of the references to color in this figure legend, the reader is referred to the web version of this article.)

5. Conclusions

In this study, the resonance of ultrasonic waves in metal-plastic bilayer laminates placed in an infinite medium has been theoretically investigated, and critical attenuation has been shown to occur in the laminates under specific conditions. Based on the viscoelastic model using the loss factor, the approximate conditions of the wave resonance and critical attenuation have been derived theoretically and compared to the exact results. For the normal wave incidence from the side of the plastic layer, it has been shown that the viscoelastic nature facilitates the wave interference, and the resonance frequencies of the plastic layer slightly increase with increasing loss factor. Nevertheless, the effect of the viscoelasticity on the resonance frequencies has not been significant if the loss factor is within the range of common plastics. On the other hand, it has been shown that the amplitude of the reflection spectrum at the resonance frequencies of the plastic layer depends on the loss factor, taking a minimum at a certain loss factor. The critical loss factors calculated by the reflection spectrum have been successfully predicted by the approximate results. Furthermore, ultrasonic measurements have been performed on two different metal-plastic bonded specimens to validate the theoretical results. The measured reflection spectra have

agreed well with the theoretical results based on the material properties obtained by other ultrasonic measurements. The drop of the amplitude at the resonance due to the critical attenuation has been successfully observed and well reproduced by the theoretical prediction.

Declaration of competing interest

The authors declare that they have no known competing financial interests or personal relationships that could have appeared to influence the work reported in this paper.

Acknowledgments

This research did not receive any specific grant from funding agencies in the public, commercial, or not-for-profit sectors.

References

[1] L.M. Brekhovskikh, Waves in Layered Media, Academic Press, New York, 1976.

[2] R.D. Borcherdt, Viscoelastic Waves in Layered Media, Cambridge University Press, Cambridge, 2009.

[3] C.C.H. Guyott, P. Cawley, Evaluation of the cohesive properties of adhesive joints using ultrasonic spectroscopy, NDT Int. 21 (1988) 233–240. https://doi.org/10.1016/0308-9126(88)90336-7.

[4] T. Pialucha, P. Cawley, The detection of thin embedded layers using normal incidence ultrasound, Ultrasonics 32 (1994) 431–440. https://doi.org/10.1016/0041-624X(94)90062-0.

[5] N.F. Haines, J.C. Bell, P.J. McIntyre, The application of broadband ultrasonic spectroscopy to the study of layered media, J. Acoust. Soc. Am. 64 (1978) 1645–1651. https://doi.org/10.1121/1.382131.

[6] R. Fiorito, W. Madigosky, H. Überall, Theory of ultrasonic resonances in a viscoelastic layer, J. Acoust. Soc. Am. 77 (1985) 489–498. https://doi.org/10.1121/1.391868.

[7] F. Simonetti, P. Cawley, Ultrasonic interferometry for the measurement of shear velocity and attenuation in viscoelastic solids, J. Acoust. Soc. Am. 115 (2004) 157–164. https://doi.org/10.1121/1.1631944.

[8] S. Dixon, B. Lanyon, G. Rowlands, Coating thickness and elastic modulus measurement using ultrasonic bulk wave resonance, Appl. Phys. Lett. 88 (2006) 141907. https://doi.org/10.1063/1.2192144.

[9] S. Dixon, B. Lanyon, G. Rowlands, Ultrasonic resonance in thin two-layer dynamic systems, J. Phys. D. Appl. Phys. 39 (2006) 506–514. https://doi.org/10.1088/0022-3727/39/3/014.

[10] A.I. Lavrentyev, S.I. Rokhlin, Ultrasonic spectroscopy of imperfect contact interfaces between a layer and two solids, J. Acoust. Soc. Am. 103 (1998) 657–664. https://doi.org/10.1121/1.423235.

514 [11] C. Han, C.T. Sun, Attenuation of stress wave propagation in periodically layered elastic
515 media, J. Sound Vib. 243 (2001) 747–761. https://doi.org/10.1006/jsvi.2000.3420.
516 [12] J. Kaplunov, A. Krynkin, Resonance vibrations of an elastic interfacial layer, J. Sound Vib.
517 294 (2006) 663–677. https://doi.org/10.1016/j.jsv.2005.11.030.
518 [13] N. Mori, N. Matsuda, T. Kusaka, Effect of interfacial adhesion on the ultrasonic interaction
519 with adhesive joints: A theoretical study using spring-type interfaces, J. Acoust. Soc. Am.
520 145 (2019) 3541–3550. https://doi.org/10.1121/1.5111856.
521 [14] R. Hodé, S. Raetz, N. Chigarev, J. Blondeau, N. Cuvillier, V. Gusev, M. Ducousso, V. Tournat,
522 Laser ultrasonics in a multilayer structure: Plane wave synthesis and inverse problem for
523 nondestructive evaluation of adhesive bondings, J. Acoust. Soc. Am. 150 (2021) 2076–2087.
524 https://doi.org/10.1121/10.0005975.
525 [15] E.V. Glushkov, N.V. Glushkova, Multiple zero-group velocity resonances in elastic layered
526 structures, J. Sound Vib. 500 (2021) 116023. https://doi.org/10.1016/j.jsv.2021.116023.
527 [16] N. Mori, D. Wakabayashi, T. Hayashi, Tangential bond stiffness evaluation of adhesive lap
528 joints by spectral interference of the low-frequency A0 Lamb wave, Int. J. Adhes. Adhes. 113
529 (2022) 103071. https://doi.org/10.1016/j.ijadhadh.2021.103071.
530 [17] A.I. Lavrentyev, S.I. Rokhlin, Anomalous attenuation effect on reflectivity of an ultrasonic
531 wave from a thin layer between dissimilar materials, J. Acoust. Soc. Am. 101 (1997) 3405–
532 3414. https://doi.org/10.1121/1.418351.
533 [18] N. Mori, Y. Iwata, T. Hayashi, N. Matsuda, Viscoelastic wave propagation and resonance in
534 a metal-plastic bonded laminate, Mech. Adv. Mater. Struct. (2022) in press.
535 https://doi.org/10.1080/15376494.2022.2084191.
536 [19] B.A. Auld, Acoustic Fields and Waves in Solids, John Wiley and Sons, New York, 1973.
537 [20] C. Bacon, B. Hosten, P.-A. Bernard, Acoustic wave generation in viscoelastic rods by time-
538 gated microwaves, J. Acoust. Soc. Am. 106 (1999) 195–201.
539 https://doi.org/10.1121/1.427073.
540 [21] M. Castaings, C. Bacon, B. Hosten, M.V. Predoi, Finite element predictions for the dynamic
541 response of thermo-viscoelastic material structures, J. Acoust. Soc. Am. 115 (2004) 1125–
542 1133. https://doi.org/10.1121/1.1639332.